J Wood Sci (2014) 60:49–58
DOI 10.1007/s10086-013-1377-8

ORIGINAL ARTICLE

Prediction of bending stiffness and moment carrying capacity of sugi cross-laminated timber

Minoru Okabe · Motoi Yasumura · Kenji Kobayashi · Kazuhiko Fujita

Received: 25 June 2013 / Accepted: 4 October 2013 / Published online: 26 November 2013

Abstract Cross-laminated timber (CLT) panels consist of several layers of lumber stacked crosswise and glued together on their faces. Prototype sugi CLT floor panels were manufactured and bending tests were carried out under the different parameters of lumber modulus of elasticity (MOE), number of layers, thickness of lumber and thickness of CLT panels. On the basis of above tests, bending stiffness and moment carrying capacity were predicted by Monte Carlo method. MOE of lumber was measured by using grading machine and tensile strength of lumber was assumed to be 60 % of bending strength based on the obtained bending test. Bending stiffness EI of CLT panels could be estimated by adopting composite theory and equivalent section area. Experimental moment carrying capacity showed 12 % higher value than the calculated moment carrying capacity by average lumber failure method, and also showed 45 % higher value than the calculated moment carrying capacity by minimum lumber failure method due to the reinforcement of the outer layer by the neighboring cross layer.

Keywords Cross-laminated timber · Composite theory · Equivalent section area · Moment carrying capacity · Monte Carlo method

Introduction

Cross-laminated timber (CLT) is produced from lumber strips that are stacked crosswise on top each other and glued with pressing to form large solid timber elements. CLT was developed in Europe few decades ago and has been growing up as industrialized engineering wood materials. Recently, CLT timber structure has been applied to large-scale multi-story buildings in Europe, which requires higher seismic and fire-resistant performance. Having not yet developed in Japan, CLT structure system might be one of the most effective solutions for the use of sugi (*Cryptomeria japonica*) from the view point of CO_2 reduction and sustainable forest management. As CLT panel is generally used for the floor panel without using horizontal members such as beams and joists, the prediction of bending stiffness and moment carrying capacity is of great importance in the design of floor elements.

In this research, prototype sugi CLT floor panels were manufactured and bending tests were carried out under the different parameters of lumber modulus of elasticity (MOE), number of layers, thickness of lumber and thickness of CLT panels. On the basis of above tests, bending stiffness and moment carrying capacity were predicted by Monte Carlo method.

Part of this article was presented at the 62th Annual Meeting of Japan Wood Research Society in Sapporo, March 2012.

M. Okabe
Tsukuba Building Research and Test Laboratory, Center for Better Living, 2 Tachihara, Tsukuba, Ibaraki 305-0802, Japan
e-mail: okabe@tbtl.org

M. Okabe
The United Graduate School of Agricultural Science, Gifu University (assigned Shizuoka University), Gifu, Japan

M. Yasumura (✉) · K. Kobayashi
Faculty of Agriculture, Shizuoka University, 836 Ohya Suruga, Shizuoka 422-8529, Japan
e-mail: afmyasu@ipc.shizuoka.ac.jp

K. Fujita
Forestry Research Center, Hiroshima Prefectural Technology Research Institute, Hiroshima 728-0013, Japan

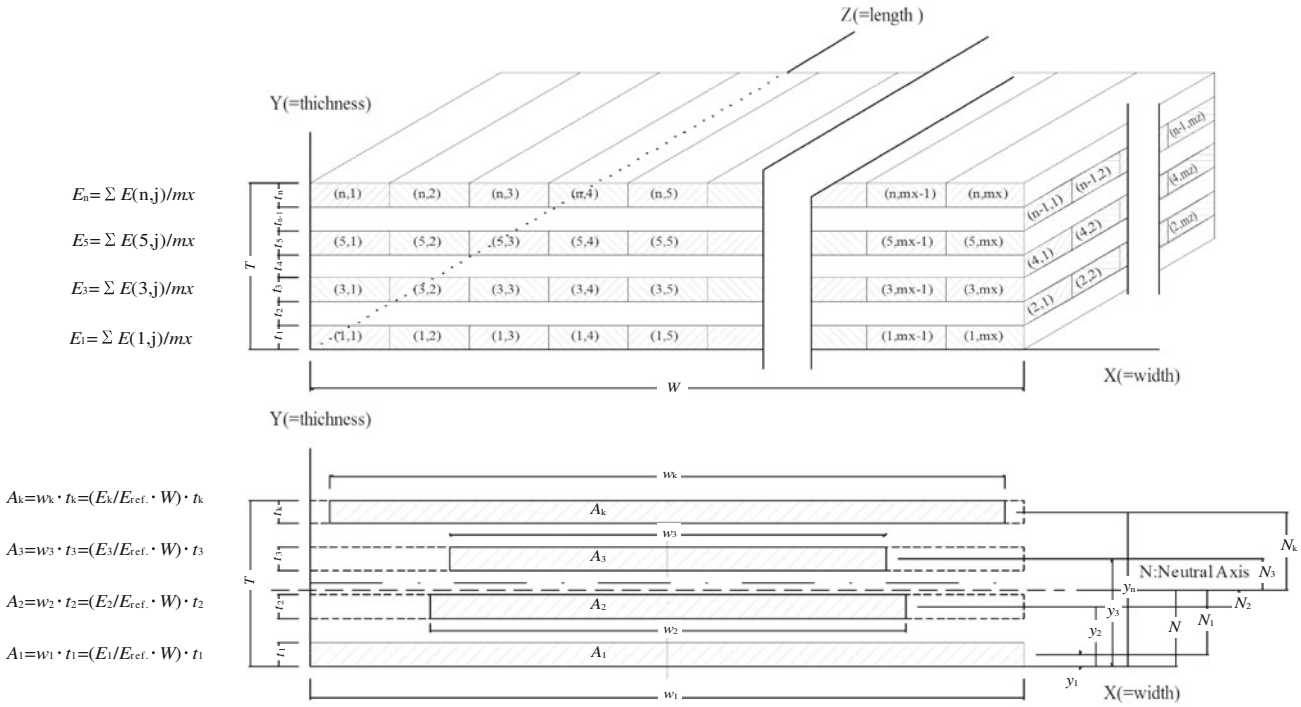

Fig. 1 Typical CLT cross-section of lumber arrangement (*W* width of CLT panels, *T* thickness of CLT panel, *n* and *mx* number of lumber in *Y* and *X* directions)

Predicting bending stiffness and moment carrying capacity of CLT panels

Modeling of lumber arrangement of CLT cross-section

Figure 1 shows the typical CLT cross-section of lumber arrangement. The variables *W*, *T* and *L* are defined CLT width, thickness and length as *X*-, *Y*- and *Z*-axis, respectively. The variable *n* is the number of layers in *Y*-direction and variable *mx* and *mz* are the number of lumber in *X*- and *Z*-direction. The variable t_i is the lumber thickness of *i*th layer and the E_i is the average MOE of lumber of *i*th layer. Main grain direction of lumber at the outer layer is parallel to the *Z* axes. Only the layers having the grain direction parallel to that of outer layers are assumed to be effective.

Equivalent width of each layer and neutral axis

Equivalent width $W_{\text{eq-}k}$ of *k*th layer is calculated in Eq. (1).

$$W_{\text{eq}-k} = W_k \times \frac{E_k}{E_{\text{ref.}}}, \tag{1}$$

where *k* is the number of effective layers [1, 2] whose grain is parallel to the longitudinal direction; $W_{\text{eq-}k}$, the equivalent width of the *k*th layer; W_k, gross width of the *k*th layer; E_k, average MOE of the *k*th layer; and E_{ref}, average MOE of reference layer.

Distance from X-axis to neutral axis is calculated in Eq. (2).

$$N = \frac{\sum_{k=1}^{n_{\text{eff}}} (W_{\text{eq}-k} \times t_k) \times Y_k}{\sum_{k=1}^{n_{\text{eff}}} (W_{\text{eq}-k} \times t_k)}, \tag{2}$$

where *N* is the distance from *X*-axis to neutral axis; Y_k, distance from *X*-axis to the centroid of the *k*th layer; and n_{eff}, number of the effective layer whose grain is parallel to the longitudinal direction.

Calculation of bending stiffness of CLT panel by composite theory

$I_{k\text{-NN}}$ shows moment of inertia of *k*th layer calculated by the composite theory (parallel layer theory) where the longitudinal direction of lumber [3, 4] in Eq. (3). Bending stiffness of CLT panel is calculated in Eq. (4).

$$I_{k-\text{NN}} = I_k + A_k \times N_k^2, \tag{3}$$

where $I_{k\text{-NN}}$ is the moment of inertia of the *k*th layer area from the neutral axes; I_k, distance from neutral axes to the centroid of each *k*th layer ($N_k = N\text{-}Y_k$); and A_k, equivalent section area multiplied $W_{\text{eq-}k}$ and t_k of the *k*th layer

$$\text{EI}_{\text{CLT}} = \sum_{k=1}^{n_{\text{eff}}} E_{\text{ref.}} \times I_{k-\text{NN}}, \tag{4}$$

where EI_{CLT} is the bending stiffness of CLT panel.

Calculation of moment carrying capacity

Moment carrying capacity of glulam is estimated by using MOE and MOR properties of lamina that compose the glulam [5–8]. Assuming that the layers are not glued each other and there is no transmission of shear forces between the layers, the bending curvature ρ of CLT panel shall be equal to that of each layer. Radius of curve $1/\rho$ and the moment of each layer are expressed in Eqs. (5) and (6).

$$\frac{1}{\rho} = \frac{M}{EI_{\mathrm{CLT}}} = \frac{M_k}{E_k I_k} \tag{5}$$

where ρ is the bending curvature ($1/\rho$: radius of curve); M, moment of CLT panel; and M_k, moment of the kth layer.

$$M_k = \frac{E_k I_k}{\mathrm{EI}_{\mathrm{CLT}}} M \tag{6}$$

when the shear stress between each effective layer is transmitted by glue, bending stress of each layer is expressed in Eq. (7).

$$\sigma_{\mathrm{b}k} = \frac{M_k}{Z_k} = \frac{I_k}{Z_k} \times \frac{E_k}{\mathrm{EI}_{\mathrm{CLT}}} \times M = \frac{t_k}{2} \times \frac{E_k}{\mathrm{EI}_{\mathrm{CLT}}} \times M, \tag{7}$$

where $\sigma_{\mathrm{b}k}$ is the bending stress of the kth layer, and Z_k, section modulus of the kth layer.

Tensile stress of each effective layer is expressed in Eq. (8).

$$\sigma_{\mathrm{t}k} = \varepsilon_k \cdot E_k = \frac{N_k}{\rho} \cdot E_k = \frac{N_k E_k}{\mathrm{EI}_{\mathrm{CLT}}} \cdot M \tag{8}$$

where $\sigma_{\mathrm{t}k}$, is the tensile stress of the kth layer and ε_k, strain due to axial force of the kth layer

Criterion for failure of CLT panel determined by the combined stress of bending and tension of lumber on each layer is expressed in Eq. (9). Moment carrying capacity $M_{\max}$ is calculated in Eq. (10) which is obtained by substituting Eqs. (7) and (8) into (9).

$$\frac{\sigma_{\mathrm{b}k}}{f_{\mathrm{b}k}} + \frac{\sigma_{\mathrm{t}k}}{f_{\mathrm{t}k}} = 1 \tag{9}$$

$$M_{\max} = \frac{\mathrm{EI}_{\mathrm{CLT}}}{E_k} \times \frac{2 f_{\mathrm{b}k} \times f_{\mathrm{t}k}}{(t_k \times f_{\mathrm{t}k} + 2 N_k \times f_{\mathrm{b}k})}, \tag{10}$$

where $f_{\mathrm{b}k}$ is the bending strength of lumber at the kth layer; and $f_{\mathrm{t}k}$, tensile strength of lumber at the kth layer

Simulation of bending stiffness and moment carrying capacity of CLT panels

MOE, bending and tensile strength of lumber

Figure 2 shows MOE distribution of sugi lumber used for CLT panels obtained by continuous grading machine (IIDA Kogyo Co., Ltd., Type MGFE-251). Average value of MOE along the longitudinal direction of lumber was obtained. MOE distribution was fitted to the two distribution curves, one is the normal probability density

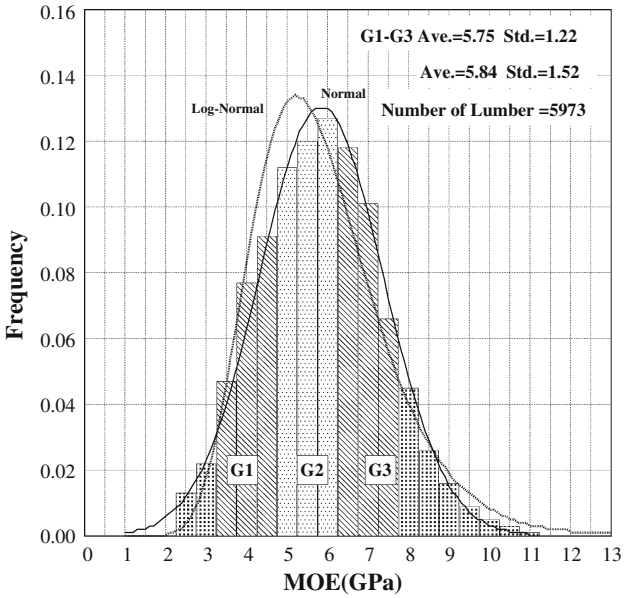

Fig. 2 Distribution of lumber MOE by grading machine

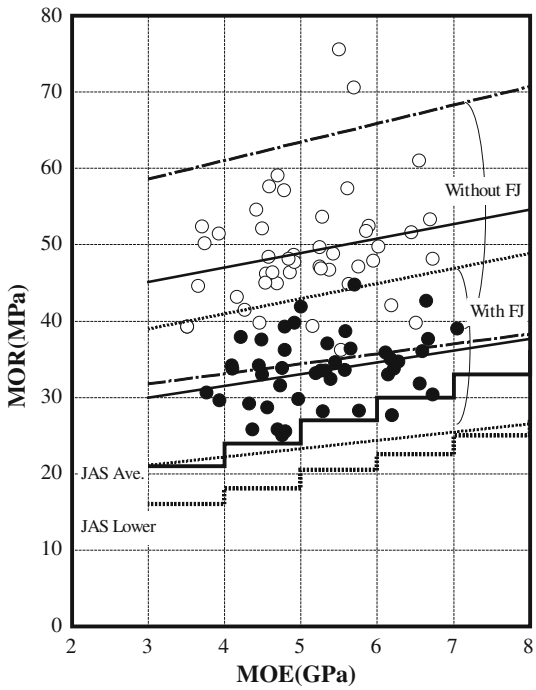

Fig. 3 Relationship between MOE and MOR of lumber by grading machine (*closed circle* with finger joint, *open circle* without finger joint). *Dashed line* 18 % COV with finger joint, *dot and dashed line* 18 % COV without finger joint, *continuous line* average value of lamina on JAS glulam, *dotted line* lower value of lamina on JAS glulam

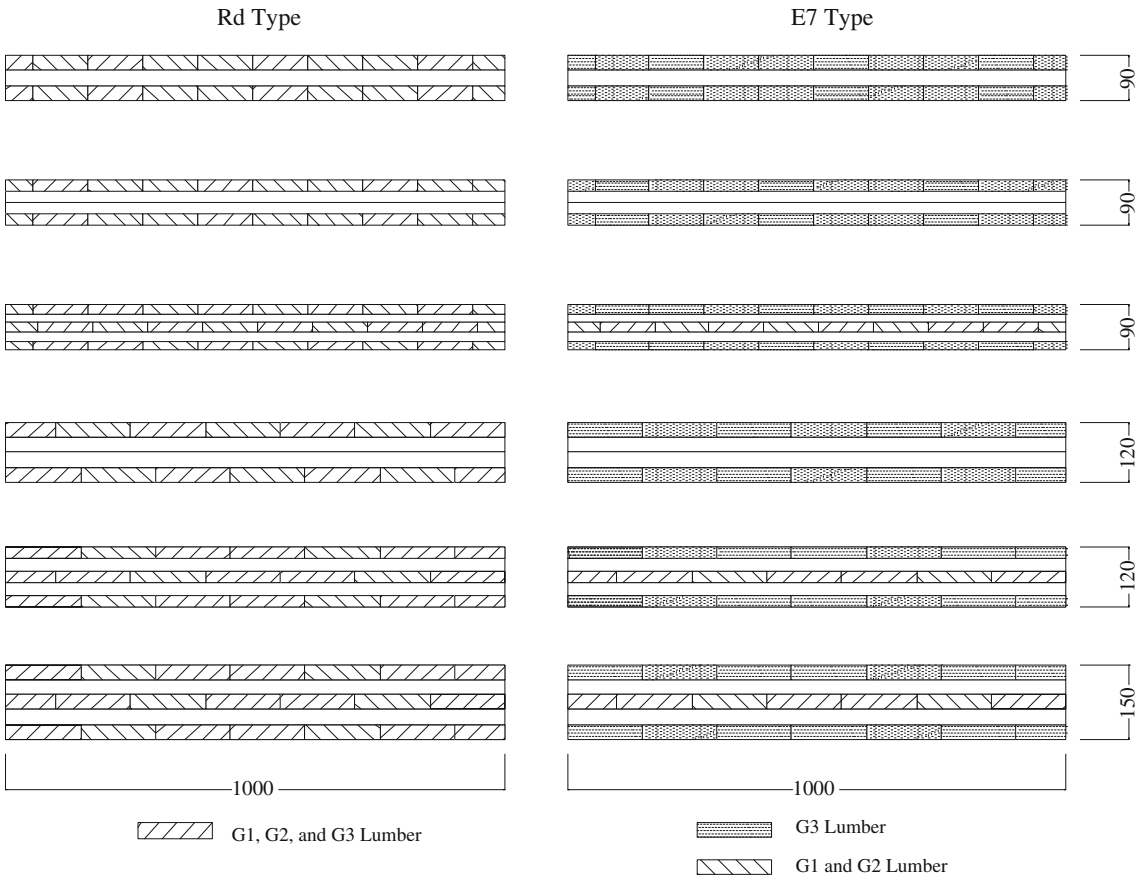

Fig. 4 Lumber arrangement of CLT cross-section

distribution curve and the other is log-normal probability density distribution curve based on the average value and standard deviation of 5973 strips of lumber. Normal distribution fitted to the distribution of lumber better than log-normal distribution. After grading, lumber was categorized to three groups according to the machine grading. Groups G1, G2 and G3 include MOE between 3.5 and 4.5 kN/mm^2, 4.5 and 6.5 kN/mm^2 and 6.5 and 8.0 kN/mm^2, respectively.

Figure 3 shows the relationship between MOE and modulus of rapture (MOR) of machine-graded lumber. MOE and MOR were determined by the bending test of lumber according to the bending method C of structural Glulam by Japanese Agricultural Standards [9]. Bending test specimen of sugi lumber was carried out on the same lot as prototype CLT panel production.

Relation between MOE and MOR showed positive correlation and MOR of lumber with finger joints showed lower value than that without finger joints. Lower and upper range assuming 18 % of COV was shown with dotted line.

Bending stiffness and moment carrying capacity by Monte Carlo method

Figure 4 shows the configuration of CLT cross-section. The configuration of simulated CLT panels matched with the manufactured CLT panels. CLT panels consisted of 1000 mm width, 3000 mm length and 3 types of thickness of 90 mm, 120 mm and 150 mm. 90-mm-thickness CLT panel had three types of layer arrangement consisting of three, four or five layers. 120-mm-thickness CLT panel had two types of layer arrangement consisting of four or five layers. 150-mm-thickness CLT panel consisted of five layers.

The layer including lumber parallel to the longitudinal direction had ten pieces of lumber in *X*-direction and the layer including of lumber perpendicular to the longitudinal direction had 28 pieces of lumber in *Z*-direction.

In E7 type of CLT panel, G3 grade of lumber was used for outer layer and G1 and G2 grades of lumber for other layers. In Rd type of CLT panel, random G1, G2 and G3 grades of lumber were used for each of the layers.

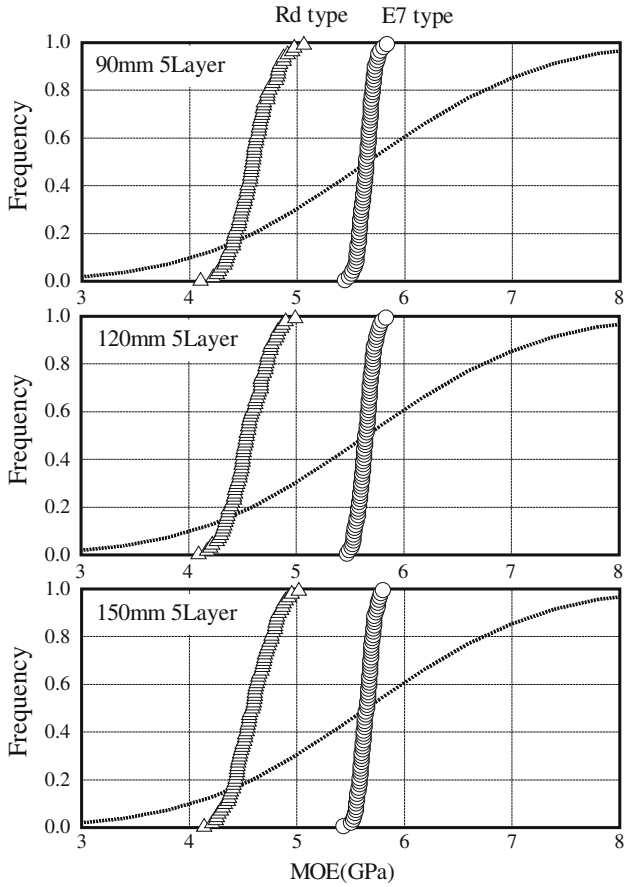

Fig. 5 Results of simulation on bending stiffness of CLT panel (*open circle* E7 type, *open square* Rd type, *dotted line* MOE of lumber)

Bending stiffness of CLT panels was simulated by Eq. (4) considering variation of lumber MOE. And moment carrying capacity was simulated by Eq. (10).

Determination method of bending stiffness and moment carrying capacity of CLT panel

Bending stiffness and moment carrying capacity of CLT panel were calculated as in the following procedure.

1. Diagram of cumulative distribution curve of normal probability density was created by the distribution of MOE lumber.
2. Average and standard deviation values of bending strength of lumber was calculated by using the relationship between MOE and MOR of lumber with finger joints, and diagram of cumulative distribution of bending strength of lumber was created from the former.
3. Assuming that tensile strength of lumber is defined by 60 % of bending strength, a diagram of cumulative distribution curve of tensile strength of lumber was created.

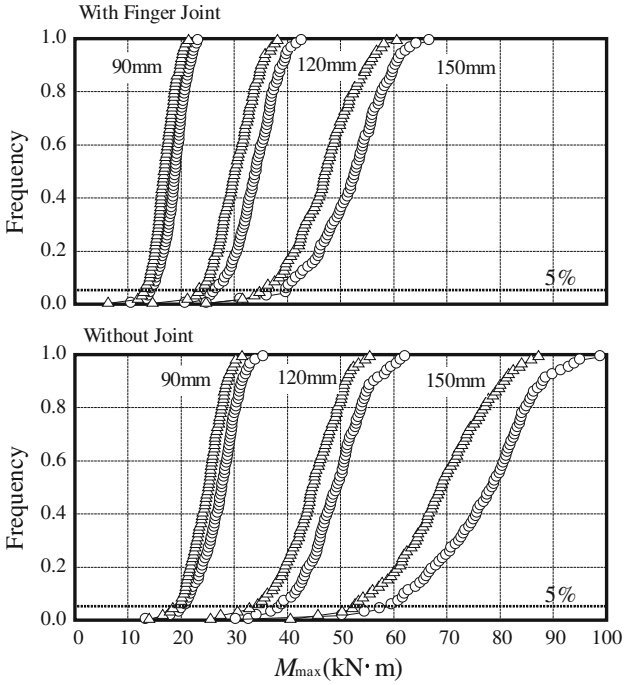

Fig. 6 Distribution of moment carrying capacity of CLT panel calculated by using minimum bending strength of lumber at the outer layer of tensile side (*open circle* E7 type, *open triangle* Rd type, *dotted line* 5th percentile lower)

4. MOE, bending and tensile strength of each lumber was chosen by Monte Carlo method using each cumulative curve, where configuration of CLT cross-section including chosen MOE, bending and tensile strength of lumber follows in Fig. 4.
5. Bending stiffness of the CLT panel was calculated by Eq. (4) of which layer's MOE was the average MOE of lumber in that layer.
6. Moment carrying capacity of CLT panel was calculated by Eq. (10) of which the outer lumber strength at the tension side was decided by the minimum bending strength among that of the particular layer (minimum strength model) or the average bending strength of the concerned layer (average strength model).

Results of simulation on bending stiffness and moment carrying capacity

Figure 5 shows the results of simulation on bending stiffness of CLT with 90, 120 and 150 mm thickness. Variation of MOE of each CLT panel showed smaller value than the variation of MOE of lumber consisted of CLT. E7 type CLT panel showed higher MOE than the Rd type CLT panel. Bending stiffness of CLT panel was affected by the MOE of lumber at the outer layer.

Figure 6 shows the distribution of moment carrying capacity of CLT panels with 90, 120 and 150 mm thickness. Moment carrying capacity was calculated by the minimum bending and tensile strengths among the lumber in the outer layer (minimum strength model).

Upper graph shows the results of simulation by the outer layer with finger joints and lower graph shows the results of simulation by the outer layer without finger joints. Maximum moment carrying capacity of CLT panel with finger joints showed lower value than the average moment carrying capacity of CLT without finger joints. However, distribution range of moment carrying capacity with finger joints was narrower than that without finger joints.

Bending test

Test specimen

Specimen of bending test was manufactured in the similar procedure as the specification of simulation for 1000 mm width, 3000 mm length and 90, 120 and 150 mm thickness. MOE of the lumber was measured by machine grading as shown in Fig. 2. Lumber arrangement of CLT cross-section was shown in Fig. 4. Water-based polymer isocyanate adhesive was used for lumber lamination and finger jointing (15 mm in length, 3.8 mm in pitch, 1/12 in slope, 0.7 mm in tip thickness. Orientation of finger joints of lumber was vertical). And no glue was applied to the edge joint of lumber on CLT manufactured. Density and moisture content of CLT panels are shown in Table 1. Moisture content of CLT panel was measured by wood moisture tester which uses the dielectric constant measuring method (Kett Electric Laboratory HM-530). Two specimens were tested for 150 and 120 mm thickness of CLT panel and only one specimen was tested for 90 mm thickness and the 90-mm-thickness CLT test specimen was measured only for stiffness of panels without failure.

Test method

Bending test was carried out according to Japan Industrial Standard JIS A 1414-2:2010 [10]. Bending test facility had a 500-kN loading capacity (Maekawa Testing Machine Mfg. Co., Ltd. Type IPU-20/100B-B1) located in Hiroshima Prefectural Technology Research Institute Forestry Research Center. Loads were applied at one-third point of 2700 mm span as shown in Fig. 7. Load was measured by load cell at the center of loading beam and vertical deflections were measured at the center and the supporting points. (Tokyo Sokki Kenkyujo Co., Ltd, SDP-100C). The average displacement at the supports was subtracted from the central displacement. The embedding displacements of CLT panels at the supports were nevertheless small. Deflection at the moment constant area was measured at the both sides of yoke equipment (Tokyo Sokki Kenkyujo Co., Ltd, CDP-50). Strains of outer layer lumber on tension and compression side were measured by strain gauge (Tokyo Sokki Kenkyujo Co., Ltd PFL-20-11-5L). Measuring position of strain gauge was shown in Fig. 8.

Loading protocol at the center deflection of span consisted of one-way cyclic loading of 1/300, 1/150, 1/100, 1/75, 1/60 and 1/50 of total span 2700 mm. Loading of 90-mm-thickness CLT panel was stopped at the deflection of 1/100 without failure.

Bending stiffness based on the deflection, bending stiffness based on moment constant deflection by yoke equipment and maximum moment were calculated by Eqs. (11), (12) and (13), respectively.

$$\mathrm{EI} = \frac{23L^3}{1296} \times \frac{\Delta P}{\Delta \delta_{\mathrm{center}}} \tag{11}$$

$$\mathrm{EI}_{\mathrm{yoke}} = \frac{L_1^3}{16} \times \frac{\Delta P}{\Delta \delta_{\mathrm{yoke}}} \tag{12}$$

$$M_{\max} = \frac{P_{\max} \times L}{6} \tag{13}$$

Table 1 Density and moisture content of CLT panels

Thickness (mm)	Layer	Arrangement of lumber	Number of specimen	Moisture content (%)	Density (kg/m^3)
150	5	Rd	2	9.1	436
				12.2	431
		E7	2	12.4	442
				15.0	431
120	4	Rd	2	11.3	442
				13.3	439
		E7	2	10.7	433
				12.8	436
	5	Rd	2	11.4	444
				10.8	439
		E7	2	12.4	436
				10.8	442
90	3	Rd	1	12.7	441
		E7	1	13.0	433
	4	Rd	1	15.3	441
		E7	1	8.1	448
	5	Rd	1	12.6	448
		E7	1	12.8	441
			Average	12.0	439
			Standard deviation	1.8	5

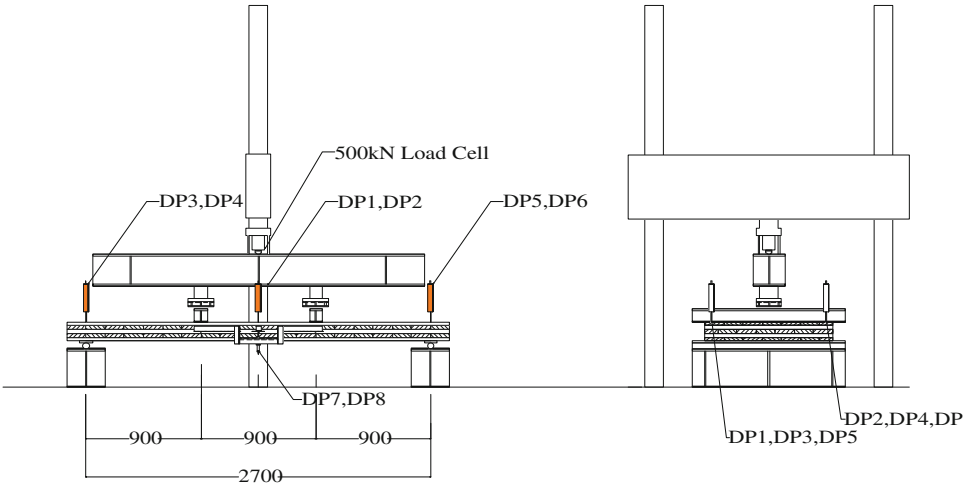

Fig. 7 Setup of the test specimen for bending (unit, mm) (setup the hard wood plate 160 × 1300 mm at loading point and steel plate 200 × 1300 mm at supporting point.)

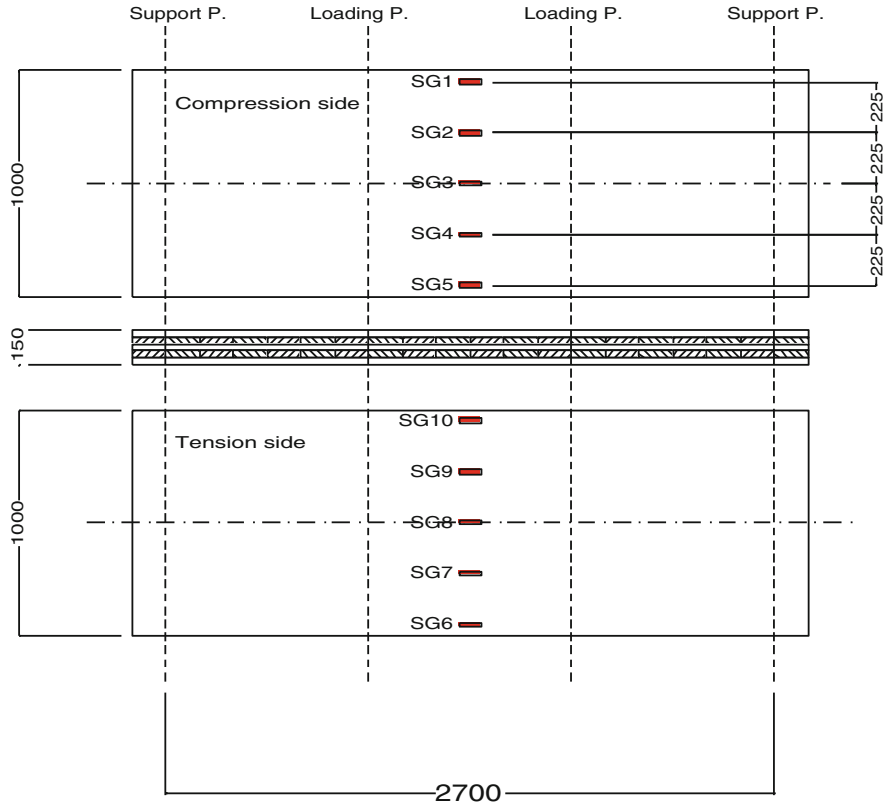

Fig. 8 Measuring position of strain by strain gauge (unit, mm)

where EI, bending stiffness on deflection by 2.7 m span (kN m^2); EI_{yoke}, bending stiffness on yoke deflection (kN m^2); ΔP, $\Delta\delta_{center}$ and $\Delta\delta_{yoke}$ are load and elastic range of deflection difference at center and yoke; L, span of bending ($L = 2.7$ m); L_1, span of bending between the moment constant area ($L_1 = 0.9$ m); M_{max}, moment carrying capacity (kN m); and P_{max}, maximum Load (kN).

Results of bending tests

Figure 9 shows the relationship between the moment and deflection of CLT panel consisted of 120 mm (5ply), 120 mm (4ply) and 150 mm (5ply). Stiffness and strength of E7 type showed higher value than the Rd type. Test results of two specimens showed almost the similar performance. Under cyclic loading below L/60 (center

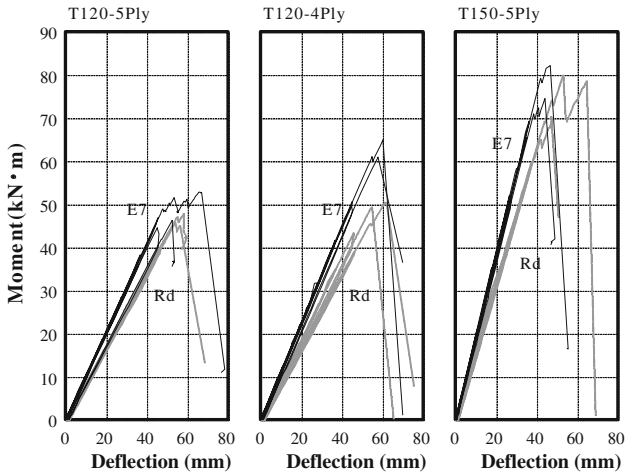

Fig. 9 Relationship between moment and deflection of bending test

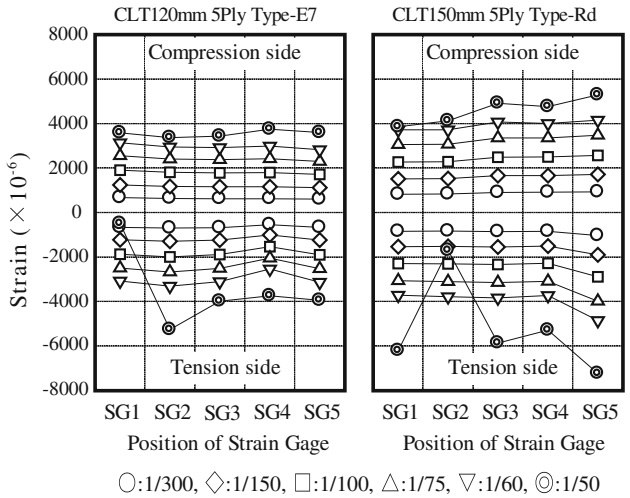

Fig. 10 Typical strain distribution of CLT panel under bending test. *Continuous line* E7 type, *dotted line* Rd type

deflection of 45 mm), reduction of stiffness of CLT panels was not observed. Typical strain distribution of CLT panel under bending test was shown in Fig. 10. Left figure shows E7 type CLT panel (120 mm and 5ply) and right figure shows Rd type CLT panel (150 mm and 5ply). Within the small deflection of $L/60$, strain distribution in X-direction of outer layer was almost constant on both tension and compression sides of CLT panel. When finger joint of certain lumber failed on the tension side of outer layer, the strains of adjacent lumber did not decrease. Another lumber of tension side next to the failed lumber shared the strain.

Figure 11 shows relationship between bending stiffness calculated by center deflection of 2700 mm span and calculated by yoke deflection. Both bending stiffness shows high correlation. Bending stiffness calculated by yoke deflection showed 8 % higher than the bending stiffness

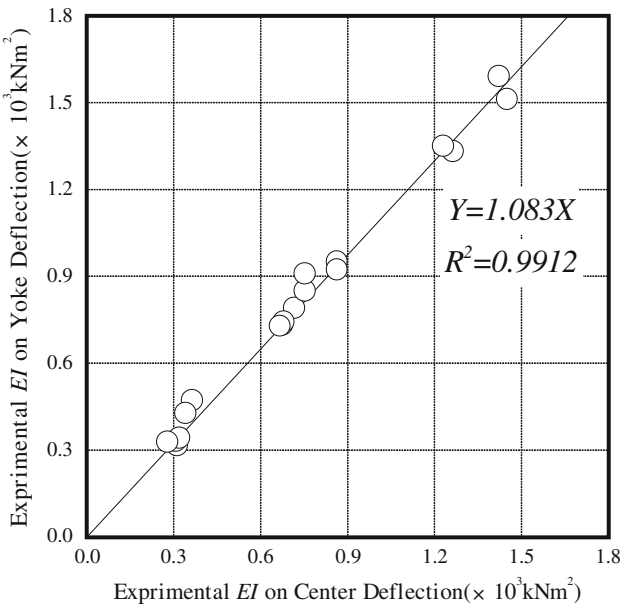

Fig. 11 Relationship between the bending stiffness based on the deflection of 2700 mm span and EI based on the yoke deflection

calculated by center deflection on 2700 mm span. It is because bending stiffness calculated by center deflection of 2700 mm span included not only bending, but also shear deflection.

Figure 12 shows typical failure of CLT panel on the tension side. At first, one of the finger joint at the tension side of constant moment area failed and then the next lumber failed due to the defects such as the finger joints, knot of lumber and cross grain continuously.

Comparison of simulation and test results

Figure 13 shows the relationship between the calculated and experimental bending stiffness. Number of calculation by Monte Carlo method was 300 on each CLT panels. Therefore, each plot shows average of calculated bending stiffness and horizontal line shows 3σ (σ, standard deviation). Circle plot and square plot shows experimental bending stiffness calculated by yoke deflection and by center deflection on 2700 mm span. Calculated bending stiffness based on the lumber MOE by grading machine with composite theory and equivalent section area was concordant with experimental bending stiffness. Experimental bending stiffness by measuring yoke deflection fitted more than the experimental bending stiffness by measuring center deflection by 2700 mm span.

Figure 14 shows the relationship between the calculated and experimental moment carrying capacity. Circle plot shows calculated moment used average strength of lumber at the outer layer on the tension side and square plot shows calculated moment used minimum strength of lumber at the

Fig. 12 Typical failure of CLT panel on tension side (type Rd 150 mm 5ply)

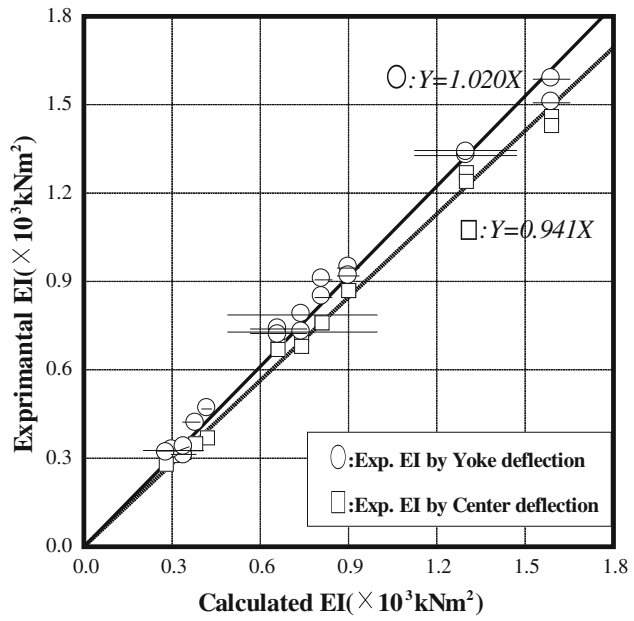

Fig. 13 Relationship between calculated and experimental EI on CLT panel

outer layer on the tension side. Experimental moment carrying capacity showed 12 % higher value than the calculated moment carrying capacity by average lumber failure method and showed 45 % higher value than the calculated moment carrying capacity by minimum lumber failure method. Those results indicate that neighboring cross layer distribute bending and tensile stress over the outer layer.

Precise prediction of moment carrying capacity of CLT panel by Monte Carlo method is effective. However, in the simulation, it is necessary to prepare the accurate lumber strength based on the MOE by grading machine. Assuming that the CLT is composed of all the minimum MOE by

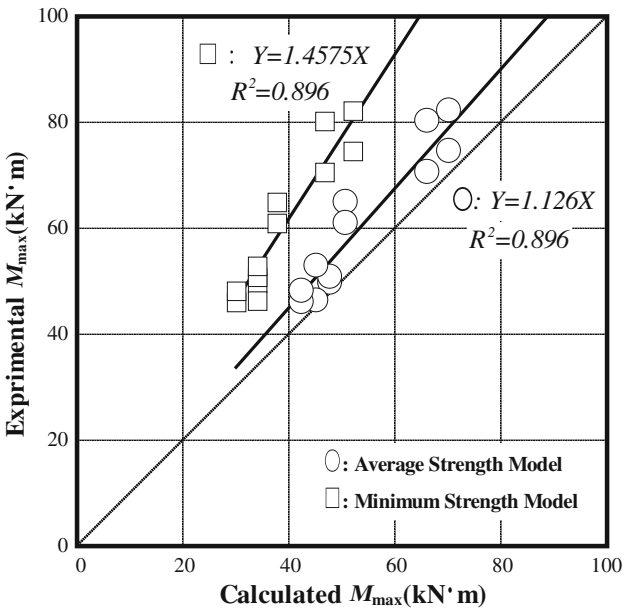

Fig. 14 Relationship between calculated and experimental maximum moment on CLT panel

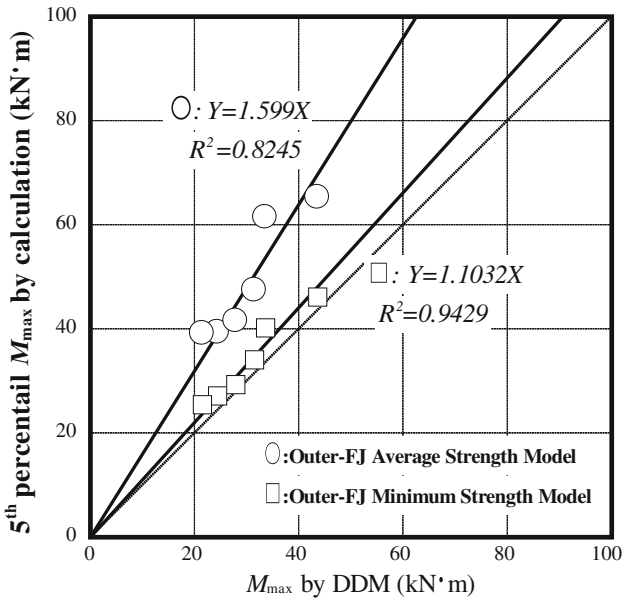

Fig. 15 Relationship between the moment carrying capacity by DDM and moment carrying capacity of 5th percentile lower by Monte Carlo method

grading, it is possible to simplify to design CLT panels. Deterministic design method (DDM) deals with the model whose MOE and MOR of all lumber in each layer is identical and based on the 5th percentile lower limit of lumber. MOE of 6.0 GPa and 22.5 MPa and 13.5 MPa for bending and tensile strength were used for E7 type of CLT panel. MOE of 3.5 GPa and 17.0 MPa and 10.2 MPa for bending and tensile strength were used for RD type of CLT panel.

Figure 15 shows the relationship between the moment carrying capacity by deterministic design method (DDM) assuming that the CLT is composed of all the minimum MOE lumber and moment carrying capacity of 5th percentile lower by Monte Carlo method. Fifth percentile moment carrying capacity by minimum strength model coincided well with the moment carrying capacity calculated by DDM. Fifth percentile moment carrying capacity by average strength model showed 1.6 times higher than both DDM and minimum strength model. Considering the simulated moment carrying capacity by average strength model was close to the experimental values in Fig. 14, DDM and minimum strength model underestimated the moment carrying capacity of CLT panel.

Conclusions

The following results were obtained in this study.

1. Bending stiffness calculated with composite theory and equivalent section area by Monte Carlo method was concordant with experimental bending stiffness.
2. Experimental moment carrying capacity showed 12 % higher value than the moment carrying capacity calculated by average strength model and showed 45 % higher value than the moment carrying capacity calculated by minimum strength model. It is supposed that the cross layer connecting each lumber of outer layer transmits the bending and tensile stress and contributes to increase the moment carrying capacity of CLT panels.
3. Within the small deflection of $L/60$, strain distribution in the lateral direction of outer layer was almost constant on both tension and compression sides of CLT panel. The fact that the strains of adjacent lumber to the failed lumber with finger joint did not decrease shows that the adjacent lumber shares the tensile and bending stress because of the existence of the cross layer.
4. Moment carrying capacity of CLT panel obtained from the 5th percentile lower limit calculated with minimum strength model was concordant with that calculated with DDM, and that obtained from the 5th percentile lower limit calculated with average strength model showed 1.6 times higher value than that calculated with DDM which was close to the experimental results. This indicates that the moment carrying capacity calculated by DDM underestimates the moment carrying capacity of CLT panel although it gives safety side design values.

Acknowledgments Test specimen of CLT panels and bending test was supported by Meiken Lamwood Corporation, and this company received the subsidy of R&D project from the Ministry of Land, Infrastructure and Transport for further prospective use to timber products. The authors would like to appreciate Mr Haramiishi, who belongs to the Meiken and also to the Japan Cross-Laminated Timber Association.

References

1. The Building Center of Japan (1988) Design and construction manual of heavy timber glulam structure (in Japanese), pp 177–184
2. FP Innovation (2011) Structural design of cross-laminated timber elements. In: CLT handbook, chap 3, pp 4–25
3. Japanese Agricultural Standards Notice No. 1751 (2008) Plywood. Ministry of Agriculture, Forestry and Fisheries
4. Sibusawa T, Nanami N, Watanabe H, Tanigawa N, Kamiya F (2002) Evaluation for mechanical performance of wood-based structural panels part 7, bending performances of relatively thicker plywood for floor sheathing predicted with parallel layer theory(in Japanese). Summaries of technical papers of Annual Meeting Architectural Institute of Japan, 22003
5. Hirashima Y, Yamamoto Y, Suzuki S (1994) Modeling for the strength of glulam beams and for their probabilistic distributions (in Japanese). Mokuzai Gakkaishi 40(11):1172–1179
6. Komatsu K (1997) Prediction of maximum bending moment of glulam beam composed of arbitrary laminae and verification by experimental results (in Japanese). Mokuzai Gakkaishi 43(11): 934–939
7. Mori T, Isoda H, Sasagawa A (2001) The proposal of the model for estimating the flexural strength of the glulam beam and verification by experimental results (in Japanese). J Struct Constr Eng Trans AIJ 541:51–57
8. Hayashi T, Itagaki N, Oguro S, Nakajima Y, Machida H (2002) Prediction of bending strength of sugi medium dimension glulam beams by monte-carlo simulation (in Japanese). J Soc Mater Sci Japan 51(4):373–378
9. Japanese Agricultural Standards Notice No. 1587 (2012) Glulam. Ministry of Agriculture, Forestry and Fisheries
10. JIS A 1414-2 (2010) Performance test methods of panel components for building construction-Part 2: tests for mechanical properties 5.3 bending test. Japan Industrial Standard, Japanese Standards Association